Haenelt, T.G.; Georgopanos, P.; Abetz, C.; Rangou, S.; Alisch, D.; Meyer, A.; Handge, U.A.; Abetz, V.:

Morphology and elasticity of polystyrene-block-polyisoprene diblock copolymers in the melt

In: Korea-Australia Rheology Journal (2014) Springer

DOI: 10.1007/s13367-014-0031-3

Morphology and elasticity of polystyrene-*block*-polyisoprene diblock copolymers in the melt

Taida Gil Haenelt[1,2], Prokopios Georgopanos[1], Clarissa Abetz[1], Sofia Rangou[1], Doreen Alisch[2], Andreas Meyer[2], Ulrich A. Handge[1,*], and Volker Abetz[1,2]

[1]*Institute of Polymer Research, Helmholtz-Zentrum Geesthacht, Max-Planck-Strasse 1, 21502 Geesthacht, Germany*

[2]*Institute of Physical Chemistry, University of Hamburg, Grindelallee 117, 20146 Hamburg, Germany*

**Corresponding author: ulrich.handge@hzg.de*

Abstract

The influence of morphology on the viscoelastic properties of melts of microphase-separated polystyrene-*block*-polyisoprene (PS-*b*-PI) diblock copolymers was investigated in oscillatory and creep recovery experiments. By means of anionic polymerization, three PS-*b*-PI diblock copolymers with a narrow molecular weight distribution and different types of morphology (spherical, cylindrical and lamellar microstructure) were prepared. Linear viscoelastic shear oscillations and creep recovery experiments in shear were performed in order to determine the elastic and viscous properties of the diblock copolymers in the melt at small and large time scales. Our analysis reveals that melts of diblock copolymers are characterized by a pronounced elastic behavior leading to a relatively large recoverable deformation in creep recovery experiments. The elasticity of the diblock copolymers is also revealed by the appearance of the creep-ringing effect. Morphological investigations were carried out to establish relations between microstructure and melt elasticity. Since ordering phenomena take place in melts of diblock copolymers until an equilibrium morphology is achieved, the storage modulus G' of diblock copolymer melts increases with time up to a steady-state value.

***Keywords*:** Diblock copolymers, microphase separation, shear rheology, creep recovery experiments, elasticity

1. Introduction

Block copolymers give rise to a variety of morphologies as they experience self-assembly based on microphase separation (Bates and Fredrickson (1990); Krappe *et al.* (1995); Breiner *et al.* (1998); Kaneko *et al.* (2006); Bates and Fredrickson (1999);Abetz and Boschetti-de-Fierro (2012)). For diblock copolymers specific microstructures can be achieved by controlling the volume fraction f and the product of χN, where χ is the Flory-Huggins interaction parameter and N the degree of polymerization (Leibler (1980); Matsen and Bates (1997); Khandpur *et al.* (1995)). The order-disorder transition (ODT) is associated with structural changes in block copolymers (Hashimoto *et al.* (1986)). Different rheological experiments were proposed by Han *et al.* (1995) to determine the order-disorder transition temperature $T_{\mathrm{ODT.}}$ The analysis of ODT was based on log G' versus log G'' plots which proved to be a very effective method.

Well-ordered block copolymers with defined microstructures have been developed for a wide range of industrial applications such as toughening using thermoplastic elastomers, membranes, high density magnetic recording devices, polymer foams and nanolithography (Park *et al.* (2003); Jung *et al.* (2012); Kryder (1992); Harrison *et al.* (2000)). Topological defects often hamper a long-range order of the morphology. It has been shown that ordering of the microstructure can be improved by an applied shear stress (Patel *et al.* (1995); Pakula *et al.* (1985); Morrison and Winter (1989)). Keller *et al.* (1970) reported on induced orientation of a cylinder forming block copolymer to almost perfect order after extrusion. Large amplitude oscillatory shear (LAOS) was employed by Koppi *et al.* (1992) in order to orient lamellar diblock copolymers. The direction of orientation is mainly influenced by temperature and by the applied shear. Only near the order-disorder transition temperature T_{ODT} the lamellar microstructure shows either a parallel or a perpendicular orientation depending on the frequency. Scott *et al.* (1992) reported on shear-induced orientation as a function of

applied strain. They concluded that large strain tends to disrupt the structure while small strains only lead to intermediate ordering. Winter *et al.* (1993) obtained a single crystal structure after quenching the sample from above the ODT and applying large-amplitude oscillatory shear flow.

Rheological experiments contribute to understand and to quantify the viscoelastic properties of polymeric materials during processing and thus are of great interest for optimizing industrial processes (Cogswell (1981)). Generally, the rheological properties are sensitive to composition, total molecular weight and chain architecture. In the absence of crosslinks, homopolymers are generally characterized by a terminal flow behavior (slopes 2 and 1 for the storage and the loss modulus as functions of frequency in double logarithmic presentations, respectively). For uncrosslinked block copolymers, a nonterminal flow behavior is reported by Larson *et al.* (1993) and Zhang and Wiesner (1998) to be an indication of a microphase separated structure. Therefore small amplitude shear oscillations are suitable for characterization of the microstructure of diblock copolymers in the melt.

A series of publications focused on the microstructural and rheological properties of polystyrene-*block*-polyisoprene (PS-*b*-PI) diblock copolymers in the melt state. The ordering dynamics of these block copolymers with polyisoprene as the major component was thoroughly investigated by Adams *et al.* (1996). A two-step increase of the storage modulus was observed in time sweep experiments. The authors interpreted the first step as a result of large-amplitude composition fluctuations and the second step as development of a body-centered-cubic (bcc) lattice. Sebastian *et al.* (2002b) studied the viscosity of diblock copolymers with a bcc morphology as a function of applied stress. Their study revealed that the steady-state viscosity strongly decreases above a critical shear stress. Furthermore the critical stress is a function of the lattice spacing and the temperature in relation to T_{ODT} (Sebastian *et al.* (2002a).) The phase behavior of various PS-*b*-PI diblock copolymers was

investigated by Förster *et al.* (1994) using transmission electron microscopy (TEM), scattering techniques and rheological experiments. Their study led to a detailed phase diagram of these diblock copolymers with a volume fraction of polyisoprene between 0.33 and 0.42.

Another type of rheological approach to compare the elastic properties of different block copolymers are creep recovery experiments (Münstedt *et al.* (2008)). For diblock copolymers, these experiments have been performed to a much lesser extent than shear oscillations. Creep recovery experiments allow for a direct determination of the recoverable part of deformation.

In this work, we analyze the influence of morphology on the elastic properties of diblock copolymers below the order-disorder transition temperature. Three different PS-*b*-PI block copolymers with different types of morphology and a roughly similar molecular weight of the polystyrene block were prepared. Linear viscoelastic shear oscillations were performed to determine the dynamic moduli as a function of time and frequency. The objective of this study is to quantify the elastic properties of diblock copolymers in the microphase separated state.

2. Experimental

2.1. Materials

Three asymmetric polystyrene-*block*-polyisoprene (PS-*b*-PI) diblock copolymers were synthesized by sequential anionic polymerization of styrene (≥ 99% with 4-*tert*-butylcatechol as stabilizer, Sigma-Aldrich, Schnelldorf) and isoprene (99% with <1000 ppm *p*-*tert*-butylcatechol as inhibitor, Sigma-Aldrich, Schnelldorf) in tetrahydrofuran using *sec*-butyllithium (1.4 M in cyclohexane, Sigma-Aldrich, Schnelldorf) as initiator. Styrene was purified over di-*n*-butylmagnesium (1.0 M in heptane, Sigma-Aldrich, Schnelldorf) and polymerized at –75 °C while isoprene was purified over *n*-butyllithium (1.6 M in hexane, Sigma-Aldrich, Schnelldorf) and polymerized at –10 °C. The synthesized diblock copolymers

are denoted by $S_uI_v^x$, where u and v correspond to the weight percent of the polystyrene and polyisoprene blocks, respectively and x corresponds to the number average molecular weight M_n in kg/mol.

2.2. Molecular characterization

The number average molecular weight M_n of the copolymers was determined by gel permeation chromatography (GPC) and ^{1}H nuclear magnetic resonance spectroscopy (^{1}H-NMR). Nuclear magnetic resonance spectra of the copolymers were recorded on a Bruker AV-300 (Bruker BioSpin GmbH, Karlsruhe, Germany) at 300 MHz using $CDCl_3$. Gel permeation chromatography was also used to calculate the polydispersity index PDI = M_w/M_n for the copolymers. All GPC measurements were performed in THF on a Waters instrument (Waters GmbH, Eschborn, Germany) with polystyrene gel columns with porosities of 10, 10^2, 10^3, 10^4 and 10^5 Å, using UV and RI detectors and polystyrene as standards. The results of the copolymer characterization are listed in Table 1.

2.3. Differential scanning calorimetry (DSC)

A differential scanning calorimeter DSC 1 (Mettler-Toledo GmbH, Gießen, Germany) was used to determine the glass transition temperature T_g of the PS and PI blocks of the diblock copolymers. The measurements were performed at 1 bar under nitrogen atmosphere and in the temperature range between –80 °C and 200 °C. The heating and cooling rates were 10 °C/min. During a first heating interval the thermal history of the PS-*b*-PI block copolymers were erased by heating up the samples from room temperature to 200 °C followed by cooling them down to –80 °C. The thermal properties were analyzed using the DSC data of the second heating interval.

2.4. Rheological experiments

2.4.1. Sample preparation

The samples for the rheological experiments were prepared by compression molding. The copolymers were pressed at 135 °C into discs with a diameter of 8 mm and a thickness of 2 mm. At the beginning, the samples were molten for 7 min without any pressure. Then vacuum was applied. After one minute a pressure of 60 kN was applied for 18 min.

2.4.2. Dynamic mechanical thermal analysis (DMTA)

The dynamic mechanical thermal properties of the copolymers were measured using a rotational rheometer (ARES, Rheometric Scientific, Piscataway (NJ), USA) in a nitrogen atmosphere. The measurements were performed at a cooling rate of 1 K/min using a plate-plate geometry with a gap of 1.9 mm. Shear response data were obtained at 1 °C intervals in the temperature range from 180 °C to 60 °C at a constant frequency of 1 Hz and a strain amplitude γ_0 of 1%.

Furthermore, DMTA experiments using the rotational rheometer MCR 502 (Anton Paar GmbH, Graz, Austria) were also carried out with the diblock copolymer $S_{86}I_{14}$[47] in order to determine the order-disorder transition temperature of this block copolymer. Cylindrical samples with a diameter of 8 mm and a gap of 1.9 mm were used for these investigations. A nitrogen atmosphere was also applied. Two different angular frequencies were applied (ω = 0.02 rad/s and ω = 0.10 rad/s). The temperature range was 250°C to 100°C. The cooling rate for these experiments was 0.5 K/min. The strain amplitude was set to γ_0 = 10%.

2.4.3. Shear rheology

Two types of dynamic oscillatory shear experiments of the PS-*b*-PI diblock copolymers were performed: isothermal time sweep and isothermal frequency sweep experiments. The

experiments were carried out using a rotational rheometer (MCR 502, Anton Paar GmbH, Graz, Austria) in a nitrogen atmosphere with a plate-plate geometry. The gap was set to 1.9 mm and the samples were allowed to equilibrate for 7 min before the experiments were started. Before each experiment oscillatory strain-sweep tests between 1% and 10% were performed at a constant angular frequency ω of 10 rad/s to determine the linear viscoelastic regime. Both, the elastic storage modulus G' and the viscous loss modulus G'' were independent of strain for the specified measurement range, so that the strain amplitude γ_0 was set to 4%. Isothermal time sweep experiments were carried out for 22500 s at a temperature T of 180 °C and an angular frequency ω of 0.1 rad/s. During isothermal frequency sweep experiments the frequency was varied between 10^{-2} and 10^{2} rad/s. The tests were started with the highest frequency (10^{2} rad/s). In order to obtain the viscoelastic properties which cover a wide range of frequencies master curves of the storage modulus G' and loss modulus G'' were obtained using the time-temperature superposition principle. Therefore shear oscillations at five different temperatures (120, 140, 160, 180 and 200 °C) were performed, with 120 °C being the reference temperature. The master curve of the sample $S_{86}I_{14}$[47] was prepared based on the temperatures between 120 °C and 180 °C, i.e. below the order-disorder transition temperature of this sample (around 184 °C). The master curves were constructed with the help of the LSSHIFT software developed by Honerkamp and Weese (1993).

2.4.4. Creep recovery experiments

Time-dependent viscoelastic properties of polymers can be also determined by creep recovery experiments in shear. The rotational rheometer (MCR 502, Anton Paar GmbH, Graz, Austria) was used for these experiments. During the creep interval a constant shear stress of 50 Pa was applied using a plate-plate geometry with a gap of 1.9 mm. The creep experiments were carried out for 10000 s at 180 °C under nitrogen flow. After the creep period the stress was set

to zero and the recoverable deformation was measured for additional 10000 s. In further creep recovery experiments, the creep stress was set to 500 Pa and to 5000 Pa, respectively.

2.5. Morphological characterization

The microstructure of compression molded samples of the diblock copolymers before and after rheological experiments were investigated by small-angle X-ray scattering (SAXS). The SAXS measurements were performed at an Incoatec X-ray source IμS with Quazar Montel optics. The wavelength was 0.154 nm. The scattering patterns were collected with a 1 x 1 mm^2 focal spot size at the sample. The sample-detector distance was 1.6 m, and the CCD-detector was a Rayonix SX165. The scattering intensity profiles were reported as the plot of the scattering intensity I vs. the magnitude of the scattering vector q, with $q = (4\pi/\lambda) \sin\theta$, where λ is the wavelength and 2θ is the scattering angle. The scattering patterns were corrected for the background before evaluations and a model with corresponding fit of the data to the corresponding microstructures was applied. These fits were included in the plot and the curves were vertically shifted for a clearer visualization.

Transmission electron microscopy (TEM) investigations were carried out using compression molded samples. Ultrathin sections were obtained by an ultramicrotome EM UC6 FCS (Leica Microsystems, Wetzlar, Germany) equipped with a diamond knife (Diatome, USA). In order to distinguish the different polymer phases, the ultrathin sections were stained with osmium tetroxide vapor. The gray domains in the TEM micrographs correspond to the PS microphase whereas the dark domains correspond to the PI microphase. The microscopic investigations were carried out using a FEI Tecnai G2 F20 (FEI, Eindhoven, The Netherlands) operated at 200 kV.

3. Results and discussion

3.1. Morphological and thermal characterization

The synthesis using the technique of anionic polymerization led to three diblock copolymers with a spherical, cylindrical and lamellar morphology (Table 1). The entanglement molecular weight M_e of polystyrene homopolymer is 18 kg/mol (Fetters *et al.* (1999)). As the molecular weight of all three polystyrene precursors of the polymerization procedure ranges between 40 and 50 kg/mol, all three diblock copolymers have around two entanglements originated from the polystyrene segments.

The morphology of the PS-*b*-PI diblock copolymer discs prepared by compression molding was studied before and after the rheological experiments (creep tests) using TEM and SAXS, see Figs. 1 to 3. As expected by the analysis of the χN values, the $S_{86}I_{14}{}^{47}$, $S_{78}I_{22}{}^{63}$ and $S_{59}I_{41}{}^{82}$ diblock copolymers microphase-separate into spherical, cylindrical and lamellar microstructure, respectively (Figs. 1 and 2). The diblock copolymers were also analyzed through SAXS measurements, and an applied model with corresponding fit confirmed these morphologies (Fig. 3). The samples in Fig. 1 were only heated during the time of compression molding above their glass transition temperature and no further annealing neither by solvent nor by temperature was carried out. This sample preparation procedure leads to incomplete relaxation processes and, as a consequence, to non-equilibrium structures (Fig. 1). It is also visible that the molecular weight of the diblock copolymers plays an important role in the size of the microstructure. As seen in the TEM micrographs, the size of the microstructures increases with molecular weight. The SAXS analysis reveals that the spheres, which have the lowest molecular weight, have also the smallest diameter of 9.8 nm while the cylinders with the intermediate molecular weight have a larger diameter of 12.4 nm. The lamellar morphology shows the largest microstructure with a lamellar spacing of 14.0 nm having at the same time the highest molecular weight and the largest fraction of polyisoprene. These results

agree with the size of the microstructure observed by transmission electron microscopy investigations.

The analysis of the transmission electron micrographs in Figs. 2(a) and (c) reveals that the morphology after the rheological creep tests (total time of creep experiment 20000 s) slightly differs from the corresponding micrographs of the samples immediately after sample preparation (Fig. 1). Generally, the diblock copolymers after the rheological experiments attained a more pronounced order. In case of the diblock copolymer with a spherical morphology ($S_{86}I_{14}^{47}$), a long-range order of the bcc lattice structure appeared (Fig. 2(a)). The interface between the PS and the PI domains in the diblock copolymer with a lamellar structure ($S_{59}I_{41}^{82}$) became significantly sharper with time, i.e. the interfacial width decreased.

Dynamic mechanical thermal analysis (DMTA) and differential scanning calorimetry (DSC) were performed to determine the glass transition temperature T_g of the diblock copolymers. During the DMTA experiments the temperature dependence of the viscoelastic moduli G' and G'' were monitored at a frequency of 1 Hz and a cooling rate of 1 K/min. The analyzed temperature interval ranged from 60 °C to 180 °C, so that only the T_g of the polystyrene block was accessible through this measurement. At low temperatures the storage modulus G' attains a high value due to predominate glassy behavior of the PS microphase of the diblock copolymers (Fig. 4). With increasing temperature the mobility of the polymer chains increases and the storage modulus G' significantly drops as the diblock copolymer softens. The glass transition temperature T_g is associated with a maximum of the loss modulus G''. At higher temperatures G'' decreases again. The storage modulus G' shows at this point a second plateau, the so-called entanglement plateau. The PS microphase of the diblock copolymers behaves as a quasi-cross-linked network. From this point forward, both moduli decrease with temperature. For the two diblock copolymers with the cylindrical and lamellar morphology,

G' is larger than G'' in the whole temperature interval. On the contrary, for the spherical morphology a cross-over of both moduli appears around 160 °C and thus the liquid-like behavior dominates this morphology at high temperatures. The T_g values for the polystyrene block are 103 °C, 105 °C and 103 °C, respectively, (Table 2) and do not depend on the morphology in agreement with literature (Rieger (1996)).

The glass transition temperature T_g was also determined by DSC, using a heating rate of 10 °C/min. In this case the analyzed temperature interval ranged from - 80 °C to 200 °C and thus was large enough to determine not only the T_g of the polystyrene block, but also the T_g of the polyisoprene block. Our analysis led to the following T_g values: - 1.2 °C, - 2.3 °C and 4.3 °C corresponding to the spherical, cylindrical and lamellar morphology, respectively. These values agree with the data of Zott and Heusinger (1975).

3.2. Isothermal time sweep experiments

Isothermal time sweep experiments of the PS-*b*-PI diblock copolymers at 180 °C and an angular frequency of 0.1 rad/s were performed to study the ordering behavior of the diblock copolymers during small amplitude oscillatory shear (SAOS). The dependence of G' and G'' as a function of time t differs for the three diblock copolymers (Fig. 5). While the dynamic moduli of the diblock copolymer with the cylindrical microstructure do not change and are thus independent of time (Fig. 5(b)), the moduli of the $S_{86}I_{14}^{47}$ diblock copolymer with the spherical microstructure show a complete different behavior (Fig. 5(a)). At the beginning, both values are roughly constant with time on the semi-logarithmic scale and attain similar values, being the loss modulus G'' slightly higher than the storage modulus G'. These data indicate a liquid-like behavior of the sample. The storage modulus increases while the loss modulus decreases, having both a crossover point at about 7500 s. The crossover time is relatively long, which shows that the thermodynamic driving force for this process is

relatively low, indicating a long-range order effect. At large times, the storage modulus is higher than the loss modulus and the sample adopts a more elastic behavior. For the diblock copolymer with the lamellar microstructure the value of the loss modulus G'' remains constant. On the contrary, the storage modulus G' increases at the beginning and tends towards a steady-state value after a short time (Fig. 5(c)). We emphasize that the increase of the storage modulus G' is not caused by chemical crosslinking of the polyisoprene phase, since our measurements were performed in a nitrogen atmosphere. Comparison of stability tests (see Fig. 6) using a polyisoprene homopolymer with M_n = 6000 g/mol reveals that polyisoprene is unstable in air (time-dependent increase of G' and G'' with time which indicates crosslinking). However, in a nitrogen atmosphere no increase of G' and G'' exists. Therefore the increase of storage modulus G' in Fig. 5 can be explained by morphological changes.

The observed time-dependence of the dynamic moduli for the diblock copolymer with a spherical morphology ($S_{86}I_{14}^{47}$) can be explained by a long-range ordering of the lattice structure. The liquid-like behavior at the beginning of the experiment is an evidence for an only incompletely ordered microstructure. Because of the mobility in the melt and possibly promoted by the small amplitude shear oscillations, the microstructure attains a more perfect order and G' increases due to the raising of a bcc structure (elastic interactions). At the end of the measurement the storage modulus G' has attained a constant value indicating the completed formation of the bcc structure. The reason why small amplitude oscillatory shear is capable to induce ordering in a spherical microstructure is that the displacement of spheres is less hindered than the displacement of cylinders and lamellae because of topological reasons. Thereby the energy barrier to displacement and orientation decreases from lamellae to cylinders to spheres.

As the crossover point appears at large times, the ordering kinetics can be considered to be slow. This result is in agreement with the works of Sebastian *et al.* (2002a); Sebastian *et al.* (2002b). The slow ordering results from the high temperature the experiment was performed at, which is just slightly below the order-disorder transition temperature T_{ODT}. At a temperature close to T_{ODT} the thermodynamic driving force for microphase separation decreases leading to a slower ordering kinetics. In order to determine precisely the order-disorder transition temperature T_{ODT}, DMTA experiments with selected parameters were performed, see Fig. 7. The temperature interval in the DMTA graphs in Fig. 7 was adjusted in order to start the measurements clearly above T_{ODT}. Furthermore, very low angular frequencies (in order to be sensitive for morphological changes) and a very low cooling rate were chosen in order to detect the order-disorder transition. The order-disorder transition is characterized by a rapid change of the slope of G' and G'' vs. T curves. Figure 7 shows such a rapid change of the slope around 184 °C. Thus we conclude $T_{ODT} \approx 184$ °C for $S_{86}I_{14}$[47].

In case of the diblock copolymer with a lamellar morphology ($S_{59}I_{41}$[82]), the interface becomes "sharper" with time which is demonstrated by the comparison of the TEM micrographs in Figs. 1(c) and 2(c). The decrease of interfacial width is caused by the incompatibility of the polystyrene and the polyisoprene blocks and the decrease of the free energy of mixing. We assume that the decrease of interfacial width with time yields an increase of the storage modulus with time.

3.3. Master curves

In order to study the time-dependent viscoelastic properties of the diblock copolymers, isothermal frequency sweep experiments were carried out at frequencies ω between 10^{-2} and 10^{2} rad/s. If those experiments are performed with thermorheologically simple homopolymers at different temperatures, the time-temperature superposition principle can be applied. Then

the values for the two dynamic moduli G' and G'' are shifted along the frequency axis. In addition, a density correction corresponding to a shift along the y axis is performed. By this way, values at higher frequencies are accessible by measurements at lower temperatures and values in the low frequency range can be obtained by measurements at higher temperatures. In case of diblock copolymers, the polymer chain consists of two types of different monomers. Therefore one cannot expect that the time-temperature superposition principle is still valid. However, because of the large mechanical contrast of the "hard" polystyrene block and the "soft" polyisoprene block, the viscoelastic behavior is determined either by the polystyrene microphase (at high frequencies) or the microphase-separated structure (at lower frequencies). Therefore we were able to apply the time-temperature superposition principle to our materials. In our experiments measurements at 120 °C, 140 °C, 160 °C, 180 °C and 200 °C (for $S_{86}I_{14}{}^{47}$ only up to 180 °C because of its T_{ODT} around 184 °C) were performed and the master curves were obtained at a reference temperature of 120 °C. The master curves of the $S_{78}I_{22}{}^{63}$ and $S_{59}I_{41}{}^{82}$ diblock copolymers (Figs. 8(b) and (c), respectively) show a similar behavior, whereas the shape of the master curve of the $S_{86}I_{14}{}^{47}$ diblock (Fig. 8(a)) differs from the other two materials.

The transition to the glassy regime can be observed for all PS-*b*-PI copolymers in the high frequency regime of the master curves. All three diblock copolymers show an entanglement plateau in the interval which can be defined by the frequencies ω_x and ω_{2x}. The entanglement plateau is larger for a larger molecular weight of the diblock copolymer. Entanglement takes place for a sufficiently high molecular weight. In this case, a quasi-cross-linked network is formed with temporarily fixed entanglement points in each microphase. As a result the storage modulus G' is larger than the loss modulus G'' in this regime, and elastic behavior of the samples dominates the viscous behavior. The entanglement average molecular weight M_e is an indicator for the length of the polymer segment between entanglements and can be

calculated for homopolymers using the concept of rubber elasticity, see the work of Ferry (1980) ,

$$G_N^0 = 4\rho RT/(5M_e) \quad (1)$$

with the polymer density ρ and the universal gas constant R. According to Ferry the plateau modulus G_N^0 can be experimentally determined as the value of G' which is associated with a minimum of the loss tangent tan δ = G'' / G'. The value of the plateau modulus G_N^0 for pure polystyrene is in the order of 2.0 x 10^5 Pa (Graessley (1980)). The value of G_N^0 for $S_{86}I_{14}{}^{47}$ nearly attains the value of pristine polystyrene. The plateau modulus of the diblock copolymers increases with polystyrene content (Table 2). Since the diblock copolymers are in the microphase-separated state with PS and PI domains, the data in the entanglement plateau result from a superposition of the dynamic moduli of both the polystyrene and the polyisoprene domains. Polyisoprene acts as a softener, since its glass transition temperature is much lower than the glass transition temperature of polystyrene, and therefore the higher polyisoprene content implies a larger fraction of the more flexible diblock copolymer domains with a lower plateau modulus than the modulus of the polystyrene domains.

In the microphase-separated state, the dynamic moduli are sensitive to the microstructure of the diblock copolymers. The crossover of G' and G'' at low frequencies can only be seen for the block copolymer with the lowest molecular weight ($S_{86}I_{14}{}^{47}$). In this case, microphase separation was not completed. Consequently, only this sample shows the beginning of the terminal regime of the Maxwell model with the power laws $G' \sim \omega^2$ and $G'' \sim \omega$. On the contrary, the diblock copolymers $S_{78}I_{22}{}^{63}$ and $S_{59}I_{41}{}^{82}$ are characterized by a plateau of the storage modulus G' at low frequencies which results from the phenomenon of microphase separation. These plateaus indicate the increase of elasticity caused by microphase separation. Ryu *et al.* (1997) observed the slope 1/3 for PS-*b*-PI diblock copolymer with PS cylinders

embedded in a PI matrix. The appearance of a plateau with a slope close to zero for our diblock copolymer shows that the matrix component (high viscous PS microphase or low viscous PI microphase) strongly influences the frequency dependence of the dynamic moduli. In contrast to the work of Zhao *et al.* (1996) and Buzza *et al.* (2000) we did not observe the slope in the order of 1/2 for the diblock copolymer with the lamellar morphology. A possible explanation is the missing long-range order of the lamellar morphology for the block copolymers of this study.

3.4. Shift factors

The shift factor a_T which results from the calculation of the master curves is presented in Fig. 9. The reference temperature T_{ref} was 120 °C. The shift factor a_T decreases with temperature T and attains similar values for all diblock copolymers of this study. For homopolymers, the shift factor can be described by the Williams-Landel-Ferry (WLF) equation which reads

$$\log(a_T) = -c_1(T - T_{\mathrm{ref}})/[c_2 + (T - T_{\mathrm{ref}})] \qquad (2)$$

with the parameters c_1 and c_2. The parameters for neat polystyrene at the reference temperature of 105 °C are given by c_1 = 12.7 and c_2 = 50 K (Ferry (1980)). Then, the shift factor a_T (T_{ref} = 120 °C) at a reference temperature of 120°C can be calculated by division of a_T (T_{ref} = 105 °C) by $a_{T\,=\,120\,^{\circ}\mathrm{C}}$ (T_{ref} = 105 °C), see Fig. 9. This result for neat polystyrene is in agreement with the shift factor for the three diblock copolymers of this study. In conclusion, at our measurement temperature the polystyrene phase strongly influences the temperature dependence of the dynamic moduli.

3.5. Creep recovery experiments

Creep recovery experiments represent another method to determine the viscoelastic properties of diblock copolymers, see, e.g., Münstedt *et al.* (2008) and Münstedt (2014). Such

experiments have been performed to a much lesser extent than experiments in the oscillatory mode. During the creep interval of such an experiment a constant shear stress is applied and the deformation of the sample as a function of time is measured. In the second part of the experiment (recovery interval), the shear stress is instantaneously set to zero and the recovered deformation of the sample is measured. In this study, the creep stress was varied in order to detect the influence of creep stress. Three different shear stress values (50 Pa, 500 Pa and 5000 Pa) were chosen. The results of the creep recovery experiments are presented in Fig. 10. The creep experiment of the $S_{86}I_{14}^{47}$ diblock copolymer with a spherical morphology yields the largest values of creep compliance $J(t)$ because of its low viscosity. Furthermore, flow processes can take place at lower stresses than in block copolymers with a cylindrical and a lamellar morphology where topological restrictions exist. When the creep stress is applied, the polystyrene blocks can slide along each other, not opposing much resistance. Furthermore, the spherical domains can rearrange to a more ordered morphology. This can be clearly seen by the more pronounced peaks of the SAXS curve after the creep recovery experiment (Fig. 3(a)). Before the creep test, only two broad reflections were present. However, after the experiment these reflections were much sharper and even a third sharp reflection was appreciable (Figs. 3(a) and (b)). A higher ordering of the morphology is also clearly visible in the TEM micrographs (Figs. 1(a) and 2(a)).

The response of the two block copolymers $S_{78}I_{22}^{63}$ and $S_{59}I_{41}^{82}$ for two different shear stress values (50 Pa and 500 Pa) are nearly equal. The creep compliance $J(t)$ monotonically increases with time, but does not attain the slope 1 at large times (Figs. 10(b) and (c)). Initially, in the time interval between 0.01 s and 1 s the creep compliance oscillates with time. This phenomenon is denoted as “creep-ringing” and is a result of the coupling of instrument inertia and sample elasticity (Ewoldt and McKinley (2007)).

In the case of the $S_{78}I_{22}^{63}$ diblock the cylinders of the polyisoprene domains have a higher aspect ratio and cannot be deformed as easily as the PI spheres and hence oppose a higher resistance to the applied stress. The creep compliance $J(t)$ also shows a monotonic increase, but the slope is much smaller and far away from unity (Figure 10(b)) as it was the case for the diblock copolymer with the spherical morphology. The number of reflections of the SAXS curve is equal before and after the rheological test, but the reflections are sharper after the experiment (Figs. 3(c) and (d)). A morphological enhancement by means of the TEM micrographs cannot be stated. The $S_{59}I_{41}^{82}$ diblock copolymer does not seem to be much affected by the experiments as there is practically no change in the values before and after the experiment. The diblock copolymers $S_{78}I_{22}^{63}$ and $S_{59}I_{41}^{82}$ are characterized by a pronounced elasticity. This is demonstrated by the time-dependent recovered creep compliances $J_r(t')$ which attain values which are almost equal to the creep compliance $J(t)$. A complete elastic (i.e. recoverable) behavior corresponds to identical values of $J(t)$ and $J_r(t')$. This elasticity of the diblock copolymer is also demonstrated by the so-called creep-ringing effect at low creep and recovery times (Fig. 10(c)).

The influence of creep stress σ_{xy} was analyzed by varying the creep stress in several creep experiments. The values of creep stress σ_{xy} were 50 Pa, 500 Pa and 5000 Pa, respectively. The results of these investigations are plotted in Fig. 11. The data indicate that at a creep stress of 500 Pa and large creep times the creep compliance $J(t)$ of the diblock copolymer with a spherical morphology ($S_{86}I_{14}^{47}$) significantly increases because of disordering of the bcc lattice structure. Such an increase is observed for the diblock copolymer with a cylindrical morphology ($S_{78}I_{22}^{63}$) only at a creep stress of 5000 Pa. On the other hand, the sample with a lamellar morphology ($S_{59}I_{41}^{82}$) seems to be quite stable at a creep stress of 5000 Pa. The variation of the creep stress shows that the mechanical stability of these diblock copolymers decreases in the order lamellae – cylinders – spheres.

4. Conclusions

In this work, the influence of morphology on the viscous and elastic properties of polystyrene-*block*-polyisoprene diblock copolymers in the melt was investigated. Our rheological experiments below the order-disorder transition temperature reveal that microphase-separated diblock copolymers are associated with pronounced elastic properties. In linear viscoelastic shear oscillations, an enhancement of long-range order of the spherical morphology leads to an increase of the storage modulus G'. A decrease of interfacial width of lamellar block copolymers also causes an increase of G'. In creep recovery experiments with a low creep stress, diblock copolymers do not attain a Newtonian flow regime with a slope of unity at large times. These experiments also reveal that diblock copolymers are associated with a recoverable part of deformation which is much larger than the corresponding value of common homopolymers. Furthermore, the variation of creep stress shows that diblock copolymers with a lamellar morphology are most stable with respect to an increase of creep stress. At our test parameters, the diblock copolymer with a cylindrical morphology can withstand a larger creep stress than the sample with a spherical morphology, but a lower creep stress than the sample with a lamellar morphology.

Acknowledgements

The authors are thankful to Ivonne Ternes for rheological experiments, Silvio Neumann for thermal analysis and nuclear magnetic resonance investigations and Maren Brinkmann for gel permeation chromatography measurements. The authors gratefully acknowledge financial support from the German Research Foundation (DFG) via SFB 986 "M3," project A2.

References

Abetz, V. and Boschetti-de-Fierro, A., 2012, Block copolymers in the condensed state, *Polymer science: a comprehensive reference* 7, 3-44.

Adams, J.L., Quiram, D.J., Graessley, W.W., Register, R.A. and Marchand, G.R., 1996, Ordering Dynamics of Compositionally Asymmetric Styrene−Isoprene Block Copolymers, *Macromolecules* 29(8), 2929-2938.

Bates, F.S. and Fredrickson, G.H., 1990, Block Copolymer Thermodynamics: Theory and Experiment, *Annual Review of Physical Chemistry* 41(1), 525-557.

Bates, F.S. and Fredrickson, G.H., 1999, Block Copolymers—Designer Soft Materials, *Print edition* 52(2), 32-38.

Breiner, U., Krappe, U., Jakob, T., Abetz, V. and Stadler, R., 1998, Spheres on spheres – a novel spherical multiphase morphology in polystyrene-block-polybutadiene-block-poly(methyl methacrylate) triblock copolymers, *Polymer Bulletin* 40(2-3), 219-226.

Buzza, D.M.A., Fzea, A.H., Allgaier, J.B., Young, R.N., Hawkins, R.J., Hamley, I.W., McLeish, T.C.B. and Lodge, T.P., 2000, Linear Melt Rheology and Small-Angle X-ray Scattering of AB Diblocks vs A2B2 Four Arm Star Block Copolymers, *Macromolecules* 33(22), 8399-8414.

Cogswell, F.N., 1981, Polymer Melt Rheology: A Guide for Industrial Practice, Elsevier Science

Ewoldt, R.H. and McKinley, G.H., 2007, Creep ringing in rheometry or how to deal with oft-discarded data in step stress tests!, *Rheol. Bull* 76(4).

Ferry, J.D., 1980, Viscoelastic Properties of Polymers, Wiley

Fetters, L.J., Lohse, D.J., Milner, S.T. and Graessley, W.W., 1999, Packing Length Influence in Linear Polymer Melts on the Entanglement, Critical, and Reptation Molecular Weights, *Macromolecules* 32(20), 6847-6851.

Förster, S., Khandpur, A.K., Zhao, J., Bates, F.S., Hamley, I.W., Ryan, A.J. and Bras, W., 1994, Complex Phase Behavior of Polyisoprene-Polystyrene Diblock Copolymers Near the Order-Disorder Transition, *Macromolecules* 27(23), 6922-6935.

Graessley, W.W., 1980, Some phenomenological consequences of the Doi–Edwards theory of viscoelasticity, *Journal of Polymer Science: Polymer Physics Edition* 18(1), 27-34.

Han, C.D., Baek, D.M., Kim, J.K., Ogawa, T., Sakamoto, N. and Hashimoto, T., 1995, Effect of volume fraction on the order-disorder transition in low molecular weight polystyrene-block-polyisoprene copolymers. 1. Order-disorder transition temperature determined by rheological measurements, *Macromolecules* 28(14), 5043-5062.

Harrison, C., Adamson, D.H., Cheng, Z., Sebastian, J.M., Sethuraman, S., Huse, D.A., Register, R.A. and Chaikin, P.M., 2000, Mechanisms of Ordering in Striped Patterns, *Science* 290(5496), 1558-1560.

Hashimoto, T., Kowsaka, K., Shibayama, M. and Kawai, H., 1986, Time-resolved small-angle x-ray scattering studies on the kinetics of the order-disorder transition of block polymers. 2. Concentration and temperature dependence, *Macromolecules* 19(3), 754-762.

Honerkamp, J. and Weese, J., 1993, A note on estimating mastercurves, *Rheola Acta* 32(1), 57-64.

Jung, A., Rangou, S., Abetz, C., Filiz, V. and Abetz, V., 2012, Structure Formation of Integral Asymmetric Composite Membranes of Polystyrene-block-Poly(2-vinylpyridine) on a Nonwoven, *Macromolecular Materials and Engineering* 297(8), 790-798.

Kaneko, T., Suda, K., Satoh, K., Kamigaito, M., Kato, T., Ono, T., Nakamura, E., Nishi, T. and Jinnai, H., 2006, A “ladder” Morphology in an ABC Triblock Copolymer, *Macromolecular Symposia* 242(1), 80-86.

Keller, A., Pedemonte, E. and Willmouth, F.M., 1970, Macro lattice from segregated amorphous phases of a three block copolymer, *Kolloid-Z.u.Z.Polymere* 238(1-2), 385-389.

Khandpur, A.K., Förster, S., Bates, F.S., Hamley, I.W., Ryan, A.J., Bras, W., Almdal, K. and Mortensen, K., 1995, Polyisoprene-Polystyrene Diblock Copolymer Phase Diagram near the Order-Disorder Transition, *Macromolecules* 28(26), 8796-8806.

Koppi, K.A., Tirrell, M., Bates, F.S., Almdal, K. and Colby, R.H., 1992, Lamellae orientation in dynamically sheared diblock copolymer melts, *J. Phys. II France* 2(11), 1941-1959.

Krappe, U., Stadler, R. and Voigt-Martin, I., 1995, Chiral Assembly in Amorphous ABC Triblock Copolymers. Formation of a Helical Morphology in Polystyrene-block-polybutadiene-block-poly(methyl methacrylate) Block Copolymers, *Macromolecules* 28(13), 4558-4561.

Kryder, M.H., 1992, Magnetic thin films for data storage, *Thin Solid Films* 216(1), 174-180.

Larson, R.G., Winey, K.I., Patel, S.S., Watanabe, H. and Bruinsma, R., 1993, The rheology of layered liquids: lamellar block copolymers and smectic liquid crystals, *Rheola Acta* 32(3), 245-253.

Leibler, L., 1980, Theory of Microphase Separation in Block Copolymers, *Macromolecules* 13(6), 1602-1617.

Matsen, M.W. and Bates, F.S., 1997, Block copolymer microstructures in the intermediate-segregation regime, *The Journal of Chemical Physics* 106(6), 2436-2448.

MORI, K., HASEGAWA, H. and HASHIMOTO, T., 1985, Small-angle X-ray scattering from bulk block polymers in disordered state. Estimation of X-values from accidental thermal fluctuations, Nature Publishing Group, Avenel, NJ, USA.

Morrison, F.A. and Winter, H.H., 1989, The effect of unidirectional shear on the structure of triblock copolymers. I. Polystyrene-polybutadiene-polystyrene, *Macromolecules* 22(9), 3533-3540.

Münstedt, H., 2014, Rheological experiments at constant stress as efficient method to characterize polymeric materials, *Journal of Rheology* 58(3), 565-587.

Münstedt, H., Katsikis, N. and Kaschta, J., 2008, Rheological Properties of Poly(methyl methacrylate)/Nanoclay Composites As Investigated by Creep Recovery in Shear, *Macromolecules* 41(24), 9777-9783.

Pakula, T., Saijo, K., Kawai, H. and Hashimoto, T., 1985, Deformation behavior of styrene-butadiene-styrene triblock copolymer with cylindrical morphology, *Macromolecules* 18(6), 1294-1302.

Park, C., Yoon, J. and Thomas, E.L., 2003, Enabling nanotechnology with self assembled block copolymer patterns, *Polymer* 44(22), 6725-6760.

Patel, S.S., Larson, R.G., Winey, K.I. and Watanabe, H., 1995, Shear Orientation and Rheology of a Lamellar Polystyrene-Polyisoprene Block Copolymer, *Macromolecules* 28(12), 4313-4318.

Rieger, J., 1996, The glass transition temperature of polystyrene, *Journal of Thermal Analysis and Calorimetry* 46(3), 965-972.

Ryu, C.Y., Lee, M.S., Hajduk, D.A. and Lodge, T.P., 1997, Structure and viscoelasticity of matched asymmetric diblock and triblock copolymers in the cylinder and sphere microstructures, *Journal of Polymer Science Part B: Polymer Physics* 35(17), 2811-2823.

Scott, D.B., Waddon, A.J., Lin, Y.G., Karasz, F.E. and Winter, H.H., 1992, Shear-induced orientation transitions in triblock copolymer styrene-butadiene-styrene with cylindrical domain morphology, *Macromolecules* 25(16), 4175-4181.

Sebastian, J.M., Lai, C., Graessley, W.W. and Register, R.A., 2002a, Steady-Shear Rheology of Block Copolymer Melts and Concentrated Solutions: Disordering Stress in Body-Centered-Cubic Systems, *Macromolecules* 35(7), 2707-2713.

Sebastian, J.M., Lai, C., Graessley, W.W., Register, R.A. and Marchand, G.R., 2002b, Steady-Shear Rheology of Block Copolymer Melts: Zero-Shear Viscosity and Shear Disordering in Body-Centered-Cubic Systems, *Macromolecules* 35(7), 2700-2706.

Winter, H.H., Scott, D.B., Gronski, W., Okamoto, S. and Hashimoto, T., 1993, Ordering by flow near the disorder-order transition of a triblock copolymer styrene-isoprene-styrene, *Macromolecules* 26(26), 7236-7244.

Zhang, Y. and Wiesner, U., 1998, Rheology of lamellar polystyrene-block-polyisoprene diblock copolymers, *Macromolecular Chemistry and Physics* 199(9), 1771-1784.

Zhao, J., Majumdar, B., Schulz, M.F., Bates, F.S., Almdal, K., Mortensen, K., Hajduk, D.A. and Gruner, S.M., 1996, Phase Behavior of Pure Diblocks and Binary Diblock Blends of Poly(ethylene)−Poly(ethylethylene), *Macromolecules* 29(4), 1204-1215.

Zott, H. and Heusinger, H., 1975, Electron Spin Resonance Investigations of Radicals and Trapped Electrons in γ-Irradiated 3,4-Polyisoprene and 1,2-Polybutadiene, *Macromolecules* 8(2), 182-185.

List of Symbols

a_T: Shift factor

f: Volume fraction

G': Storage modulus

G'': Loss modulus

G_N^0: Plateau modulus

I: Scattering intensity

$J(t)$: Creep compliance

$J_r(t')$: Recovered creep compliance

M_e: Entanglement molecular weight

M_n: Number average of the molecular weight

M_w: Mass average of the molecular weight

N: Degree of polymerization

PDI: Polydispersity index

q: Magnitude of the scattering vector

R: Universal gas constant

t: Time

t': Recovery time

t_{max}: Creep time

T: Temperature

T_g: Glass transition temperature

T_{ODT}: Order-disorder transition temperature

T_{ref}: Reference temperature

γ_0: Strain amplitude

tan δ: Loss tangent

λ: Wavelength

ρ: Density

θ: Half of the scattering angle

χ: Flory-Huggins interaction parameter

σ_{xy}: Creep stress

ω: Angular frequency

Table Captions

Table 1: Results of characterization of the diblock copolymers of this study.

Table 2: Results of thermal characterization of the diblock copolymers of this study.

Table 3: Parameters describing the entanglement regime in linear viscoelastic shear oscillations.

Figure Captions:

Figure 1: Transmission electron micrographs of compression molded and stained, ultra-thin cross sections of the (a) spherical diblock copolymer $S_{86}I_{14}^{47}$, (b) cylindrical diblock copolymer $S_{78}I_{22}^{63}$ and (c) lamellar diblock copolymer $S_{59}I_{41}^{82}$. The white phase corresponds to the PS phase and the black one to the PI phase.

Figure 2: Transmission electron micrographs of compression molded and stained, ultra-thin cross sections of the (a) spherical diblock copolymer $S_{86}I_{14}^{47}$, (b) cylindrical diblock copolymer $S_{78}I_{22}^{63}$ and (c) lamellar diblock copolymer $S_{59}I_{41}^{82}$ after a creep test with σ_{xy} = 50 Pa (creep time 10000 s, recovery time 10000 s). The white parts correspond to the PS phase and the black one to the PI phase.

Figure 3: Results of SAXS measurements showing the intensity *I* as a function of the magnitude of the scattering vector *q* before and after creep recovery experiments of (a) spherical ($S_{86}I_{14}^{47}$), (b) cylindrical ($S_{78}I_{22}^{63}$) and (c) lamellar ($S_{59}I_{41}^{82}$) diblock copolymers. The curves are vertically shifted for a clearer visualization.

Figure 4: Storage modulus *G'* and loss modulus *G"* as a function of temperature *T* at a frequency of 1 Hz. The cooling rate was 1 K/min, and the strain amplitude was γ_0 = 1%. The diblock copolymers are (a) $S_{86}I_{14}^{47}$, (b) $S_{78}I_{22}^{63}$ and (c) $S_{59}I_{41}^{82}$.

Figure 5: Additional DMTA investigations for the diblock copolymer $S_{86}I_{14}^{47}$ at two different angular frequencies for determination of the order-disorder transition temperature. The cooling rate was 0.5 K/min, and the strain amplitude γ_0 = 10%. The angular frequency ω is indicated.

Figure 6: Results of stability tests: Storage and loss modulus *G'* and *G"* as a function of time *t* at 180 °C for the (a) spherical diblock copolymer $S_{86}I_{14}^{47}$, (b) cylindrical diblock copolymer $S_{78}I_{22}^{63}$ and (c) lamellar diblock copolymer $S_{59}I_{41}^{82}$.

Figure 7: Stability curves of *G'* and *G"* as a function of time *t* at 180 °C for polyisoprene with M_n = 6000 kg/mol measured in air and in nitrogen atmosphere**,** respectively.

Figure 8: Master curves of *G'* and *G"* as a function of angular frequency ω for the (a) spherical diblock copolymer $S_{86}I_{14}^{47}$, (b) cylindrical diblock copolymer $S_{78}I_{22}^{63}$ and (c) lamellar diblock copolymer $S_{59}I_{41}^{82}$. The shift factor is denoted by a_T. The reference temperature is 120 °C.

Figure 9: Shift factor a_T as a function of temperature *T* for (a) spherical diblock copolymer $S_{86}I_{14}^{47}$, (b) cylindrical diblock copolymer $S_{78}I_{22}^{63}$ and (c) lamellar diblock copolymer $S_{59}I_{41}^{82}$ and a polystyrene homopolymer. The shift factor for homopolystyrene was calculated using the WLF equation with the parameters c_1 = 12.7 and c_2 = 50 K. The reference temperature is 120 °C.

Figure 10: Creep compliance *J(t)* and recovered creep compliance $J_r(t')$ of the (a) spherical diblock copolymer $S_{86}I_{14}^{47}$, (b) cylindrical diblock copolymer $S_{78}I_{22}^{63}$ and (c) lamellar diblock copolymer $S_{59}I_{41}^{82}$ diblock copolymer as a function of time *t* and recovery time *t'*, respectively. The value of creep stress σ_{xy} was 50 Pa and 500 Pa, respectively. The creep time t_{max} was 10000 s. The measurement temperature was 180 °C.

Figure 11: Influence of creep stress σ_{xy} on the creep compliance $J(t)$ in the creep interval for the three diblock copolymers of this study. The value of σ_{xy} is indicated for each diblock copolymer. The sample with a lamellar morphology appears to be most stable. The creep time was 10000 s and the measurement temperature 180 °C.

Tables

Table 1. Results of characterization of the diblock copolymers of this study.

Polymer	PDI	χN	Morphology
$S_{86}I_{14}^{47}$	1.15	36[c)]	Spherical
$S_{78}I_{22}^{63}$	1.08	50[c)]	Cylindrical
$S_{59}I_{41}^{82}$	1.08	71[c)]	Lamellar

$S_uI_v^x$, where u and v correspond to the weight percent of the components and x corresponds to the number average molecular weight M_n in kg/mol.
χN calculated according to c) MORI *et al.* (1985)

Table 2. Results of thermal characterization of the diblock copolymers of this study.

	DSC		DMTA
Polymer	T_g(PI) [°C]	T_g(PS) [°C]	T_g(PS) [°C]
$S_{86}I_{14}^{47}$	-1.2	97.76	103
$S_{78}I_{22}^{63}$	-2.3	95.86	105
$S_{59}I_{41}^{82}$	4.3	99.10	103

Table 3. Parameters describing the entanglement regime in linear viscoelastic shear oscillations.

Polymer	G_N^0 [Pa]	ω_x [rad/s]	ω_{2x} [rad/s]
$S_{86}I_{14}^{47}$	1.0×10^5	2.5×10^{-3}	1.3
$S_{78}I_{22}^{63}$	9.6×10^4	3.3×10^{-4}	1.3
$S_{59}I_{41}^{82}$	5.8×10^4	7.0×10^{-5}	3.1
Polystyrene[a)]	2.0×10^5		

a) Graessley (1980)

Figures

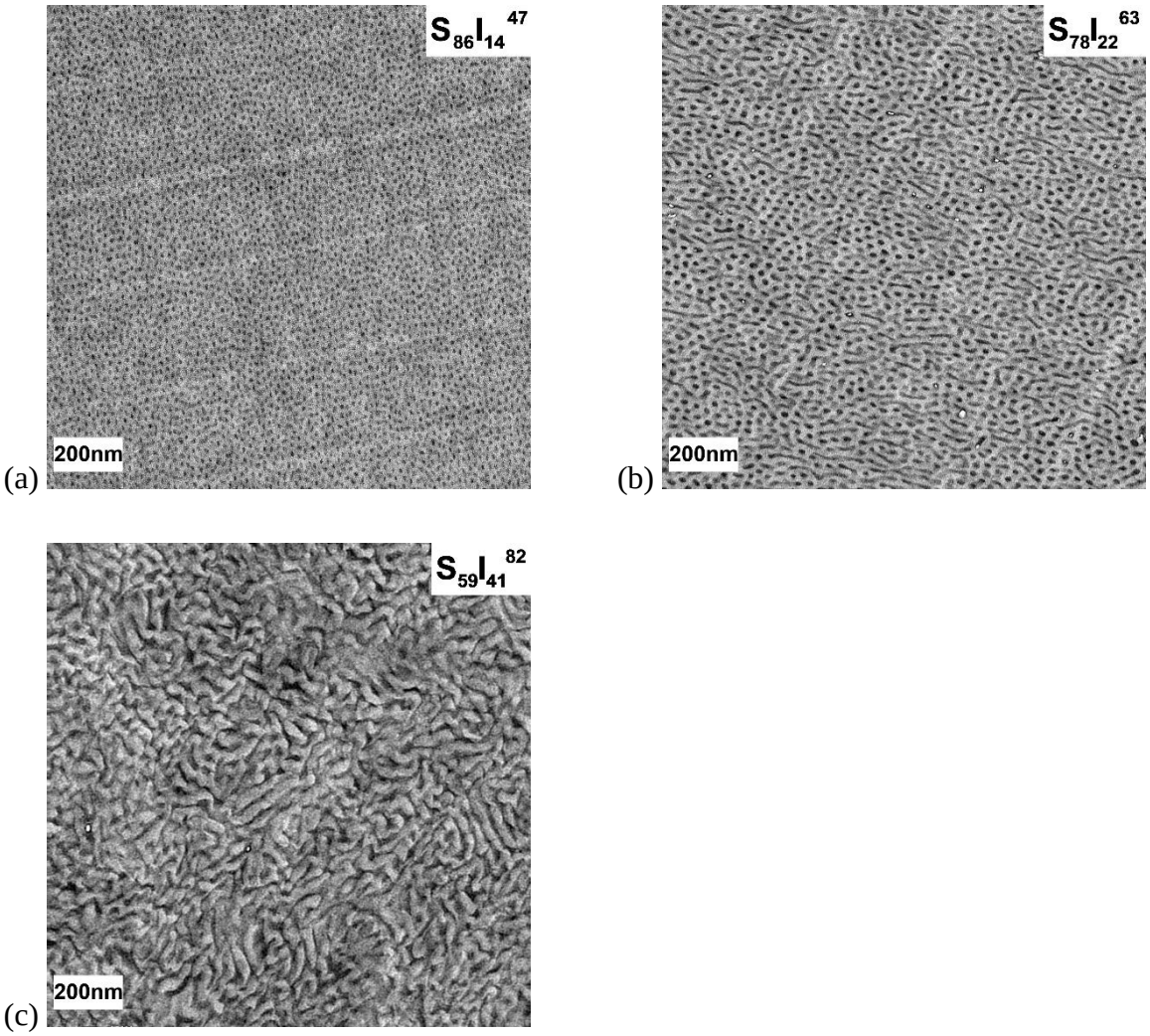

Figure 1. Transmission electron micrographs of compression molded and stained, ultra-thin cross sections of the (a) spherical diblock copolymer $S_{86}I_{14}^{47}$, (b) cylindrical diblock copolymer $S_{78}I_{22}^{63}$ and (c) lamellar diblock copolymer $S_{59}I_{41}^{82}$. The white phase corresponds to the PS phase and the black one to the PI phase.

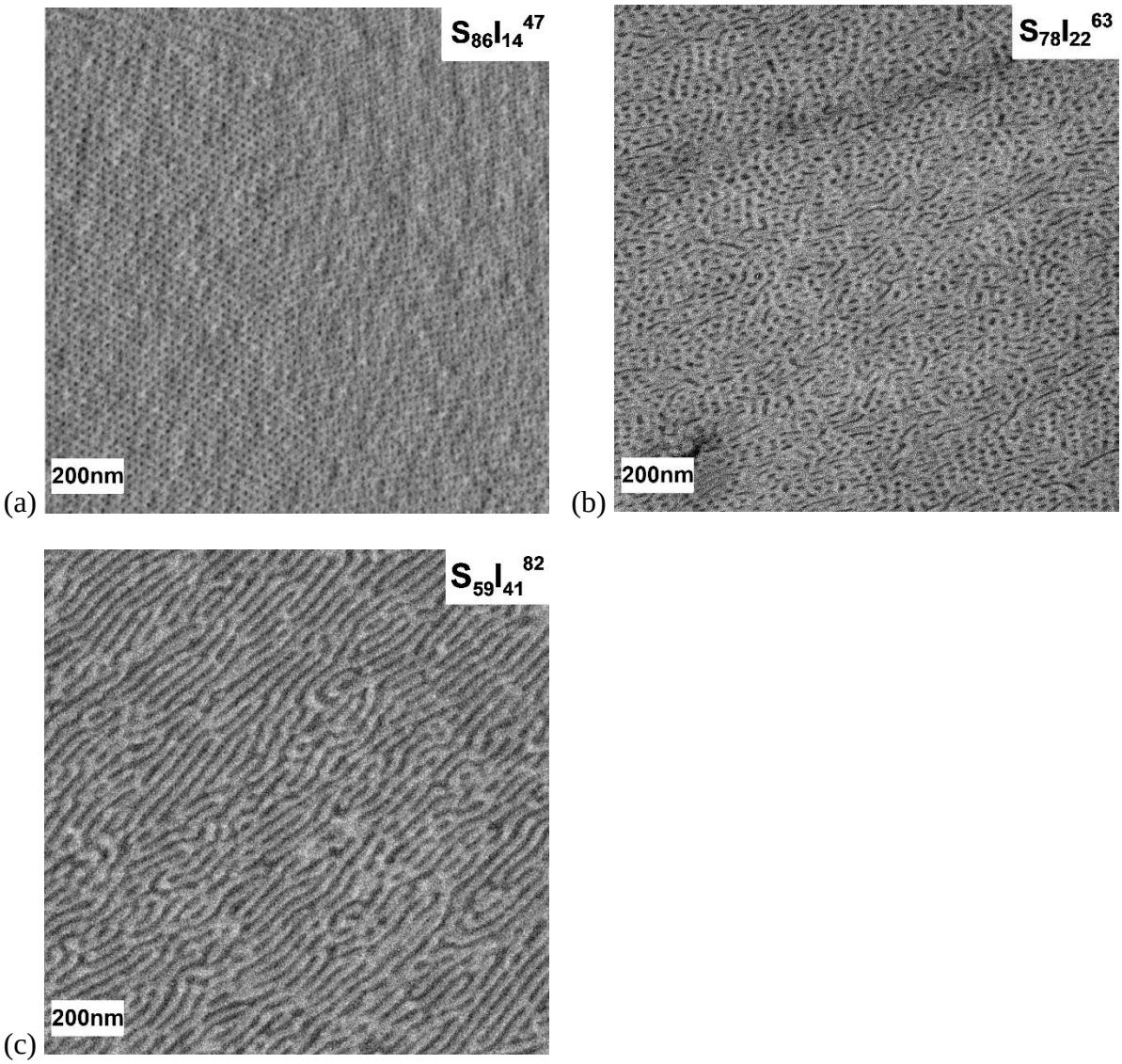

Figure 2. Transmission electron micrographs of compression molded and stained, ultra-thin cross sections of the (a) spherical diblock copolymer $S_{86}I_{14}{}^{47}$, (b) cylindrical diblock copolymer $S_{78}I_{22}{}^{63}$ and (c) lamellar diblock copolymer $S_{59}I_{41}{}^{82}$ after a creep test with σ_{xy} = 50 Pa (creep time 10000 s, recovery time 10000 s). The white parts correspond to the PS phase and the black one to the PI phase.

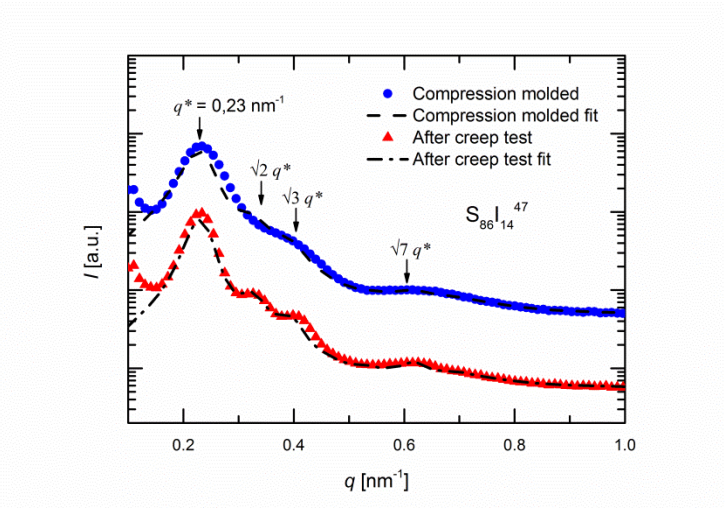

(a)

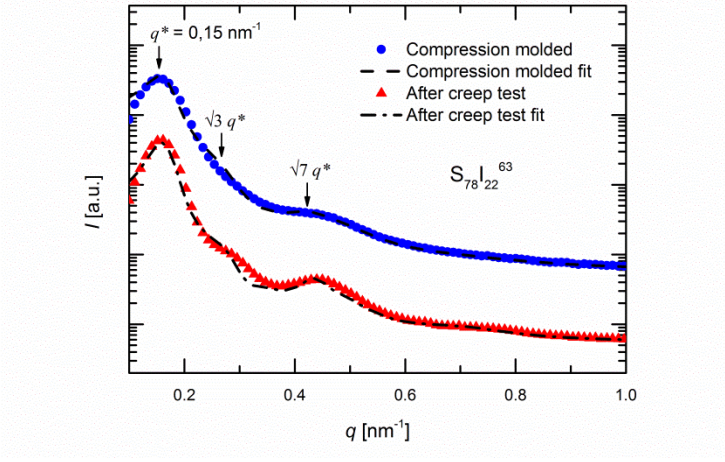

(b)

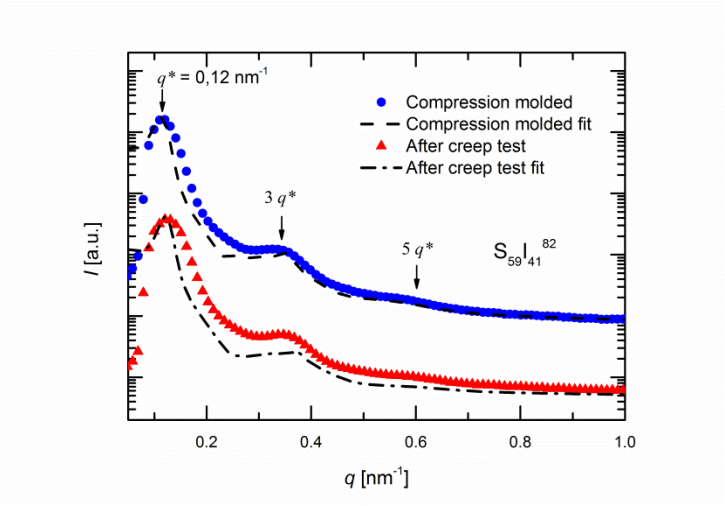

(c)

Figure 3. Results of SAXS measurements showing the intensity *I* as a function of the magnitude of the scattering vector *q* before and after creep recovery experiments of (a) spherical ($S_{86}I_{14}^{47}$), (b) cylindrical ($S_{78}I_{22}^{63}$) and (c) lamellar ($S_{59}I_{41}^{82}$) diblock copolymers. The curves are vertically shifted for a clearer visualization.

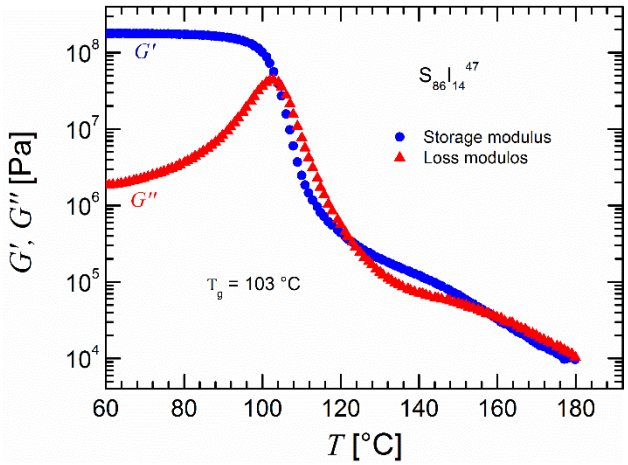

(a)

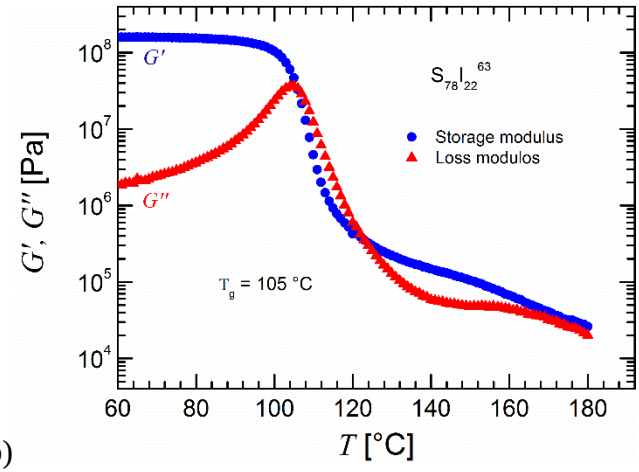

(b)

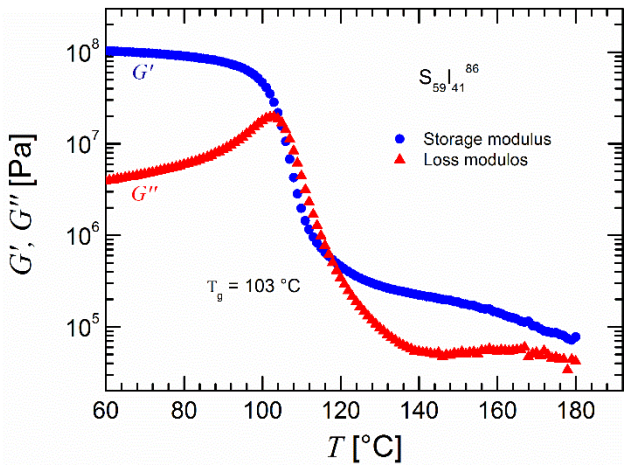

(c)

Figure 4. Storage modulus G' and loss modulus G'' as a function of temperature T at a frequency of 1 Hz. The cooling rate was 1 K/min, and the strain amplitude was γ_0 = 1%. The diblock copolymers are (a) $S_{86}I_{14}{}^{47}$, (b) $S_{78}I_{22}{}^{63}$ and (c) $S_{59}I_{41}{}^{82}$.

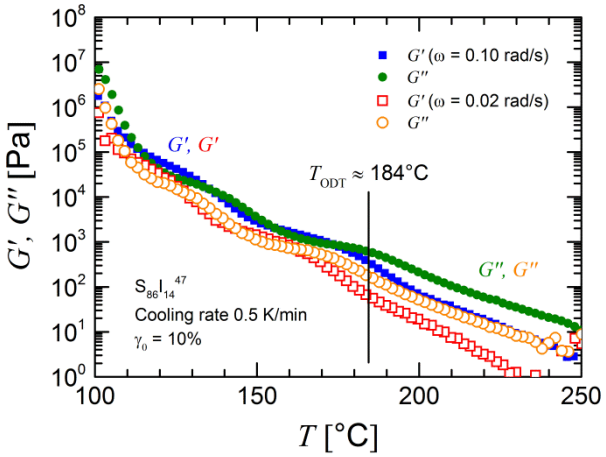

Figure 5. Additional DMTA investigations for the diblock copolymer $S_{86}I_{14}{}^{47}$ at two different angular frequencies for determination of the order-disorder transition temperature. The cooling rate was 0.5 K/min, and the strain amplitude γ_0 = 10%. The angular frequency ω is indicated.

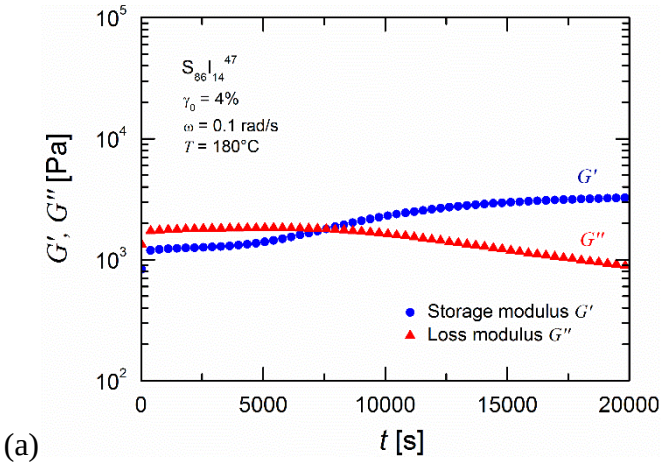

(a)

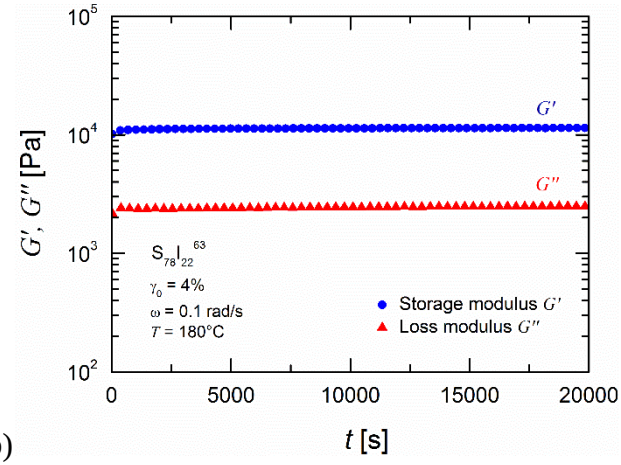

(b)

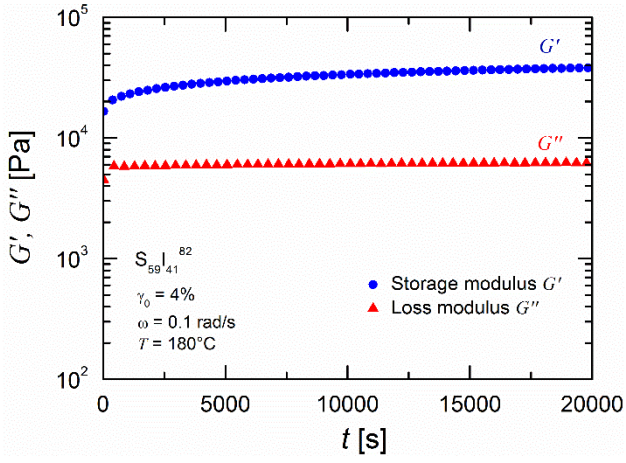

(c)

Figure 6. Results of stability tests: Storage and loss modulus G' and G'' as a function of time t at 180 °C for the (a) spherical diblock copolymer $S_{86}I_{14}^{47}$, (b) cylindrical diblock copolymer $S_{78}I_{22}^{63}$ and (c) lamellar diblock copolymer $S_{59}I_{41}^{82}$.

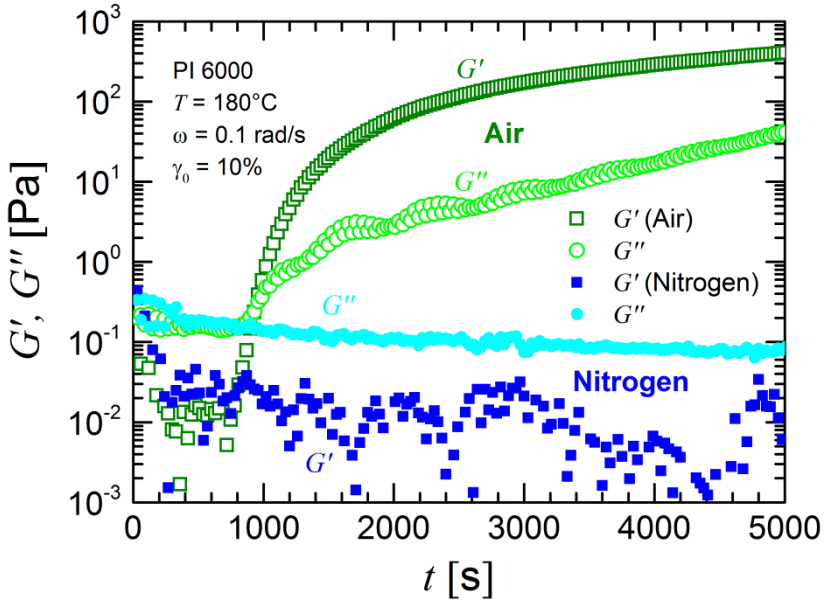

Figure 7. Stability curves of G' and G'' as a function of time t at 180 °C for polyisoprene with M_n = 6000 kg/mol measured in air and in nitrogen atmosphere**,** respectively.

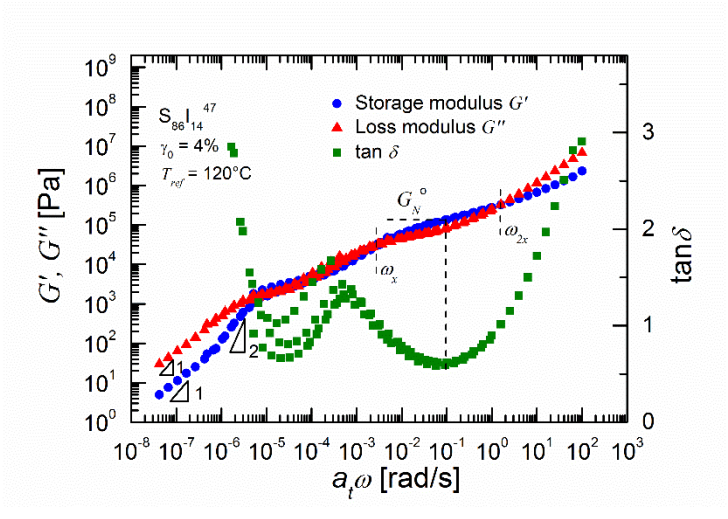

(a)

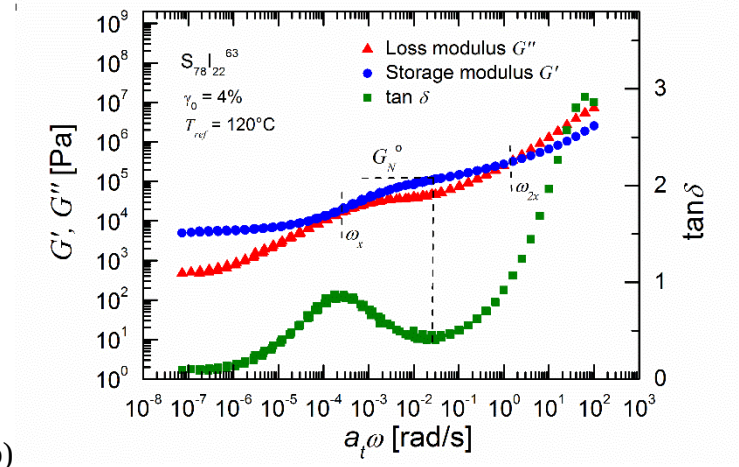

(b)

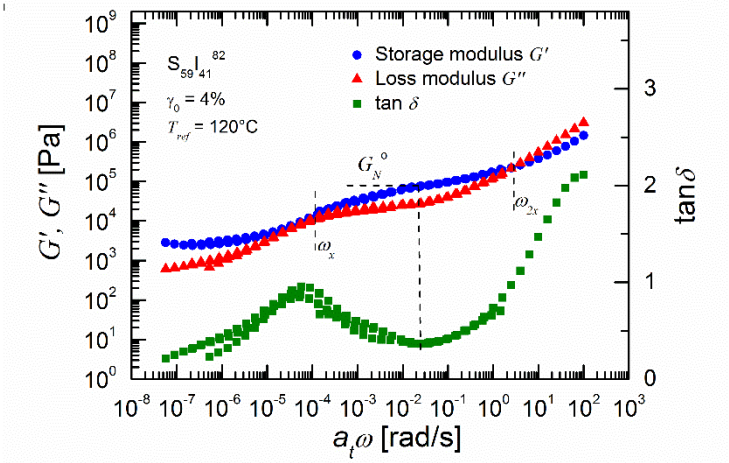

(c)

Figure 8. Master curves of G' and G'' as a function of angular frequency ω for the (a) spherical diblock copolymer $S_{86}I_{14}{}^{47}$, (b) cylindrical diblock copolymer $S_{78}I_{22}{}^{63}$ and (c) lamellar diblock copolymer $S_{59}I_{41}{}^{82}$. The shift factor is denoted by a_T. The reference temperature is 120 °C.

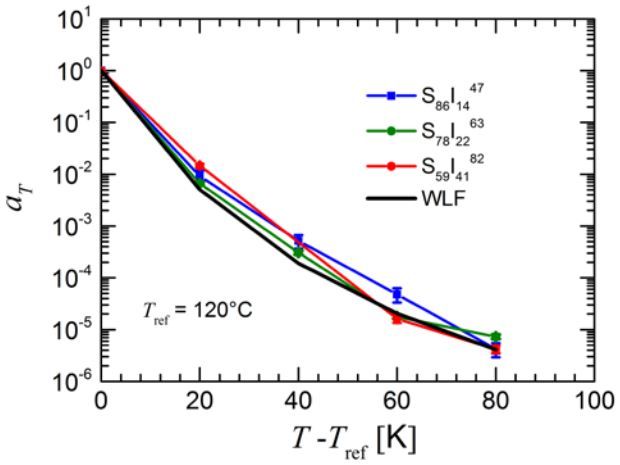

Figure 9. Shift factor a_T as a function of temperature T for (a) spherical diblock copolymer $S_{86}I_{14}{}^{47}$, (b) cylindrical diblock copolymer $S_{78}I_{22}{}^{63}$ and (c) lamellar diblock copolymer $S_{59}I_{41}{}^{82}$ and a polystyrene homopolymer. The shift factor for homopolystyrene was calculated using the WLF equation with the parameters c_1 = 12.7 and c_2 = 50 K. The reference temperature is 120 °C.

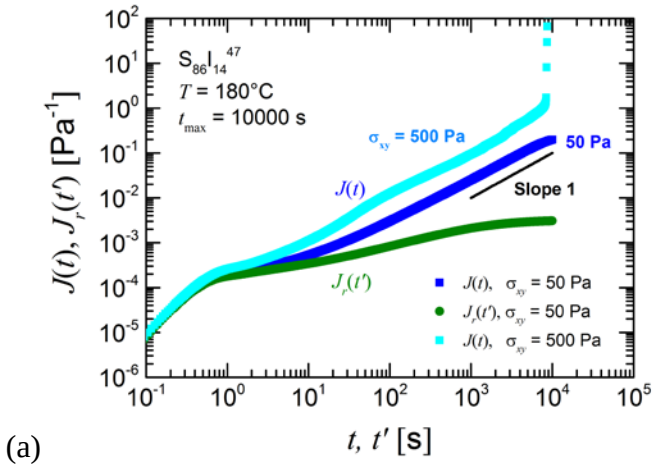

(a)

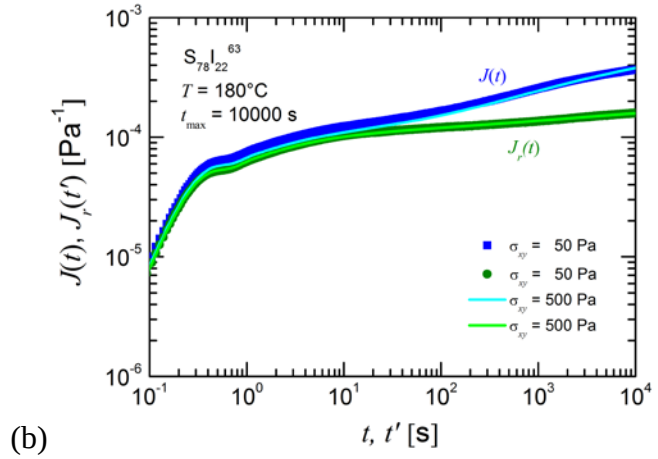

(b)

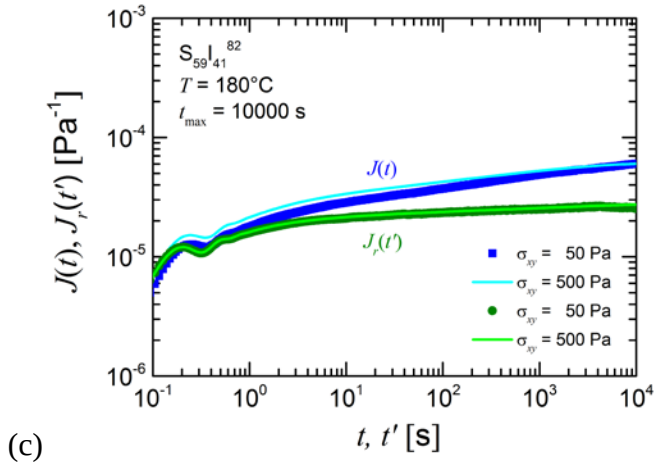

(c)

Figure 10. Creep compliance *J(t)* and recovered creep compliance $J_r(t')$ of the (a) spherical diblock copolymer $S_{86}I_{14}{}^{47}$, (b) cylindrical diblock copolymer $S_{78}I_{22}{}^{63}$ and (c) lamellar diblock copolymer $S_{59}I_{41}{}^{82}$ diblock copolymer as a function of time t and recovery time t', respectively. The value of creep stress σ_{xy} was 50 Pa and 500 Pa, respectively. The creep time t_{max} was 10000 s. The measurement temperature was 180 °C.

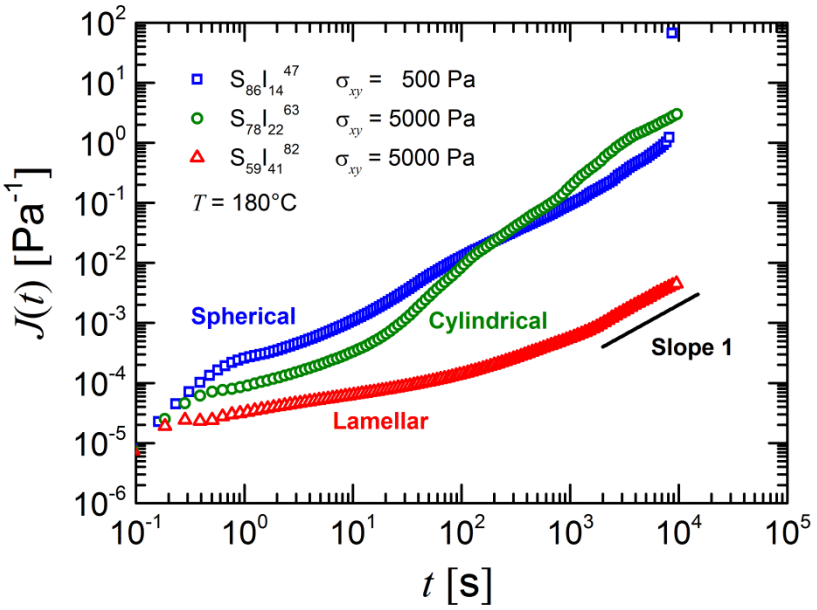

Figure 11. Influence of creep stress σ_{xy} on the creep compliance $J(t)$ in the creep interval for the three diblock copolymers of this study. The value of σ_{xy} is indicated for each diblock copolymer. The sample with a lamellar morphology appears to be most stable. The creep time was 10000 s and the measurement temperature 180 °C.